

Showcase 3 - DEMO3.2 and Showcase 4 - DEMO4.2 (D2.3 - SGA3)

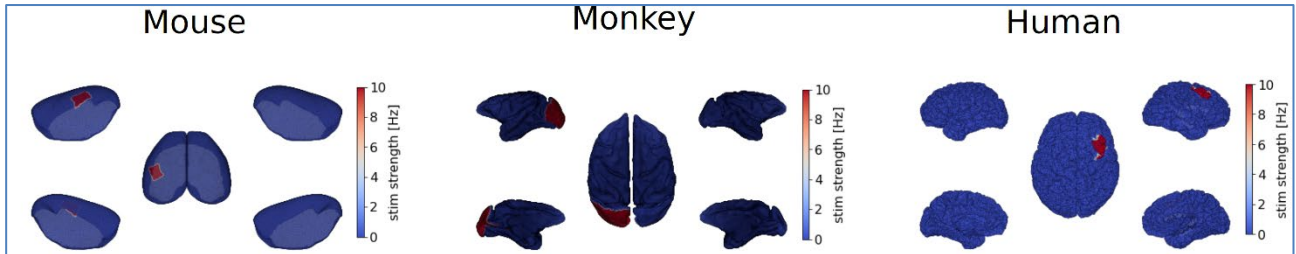


Figure 1: Showcase 3 - Simulation of brain states in mouse, macaque and human. Whole-brain simulations of wake-like (conscious) and anaesthesia (unconscious) states in three different species.

Showcase 3 present simulations of spontaneous activity, together with results about brain responses to external stimuli in those brain states. Simulations were done in TVB using the integration of AdEx mean-field models developed previously and were implemented on EBRAINS. A new framework of surface-based simulations is also presented, giving access to more accurate simulations.

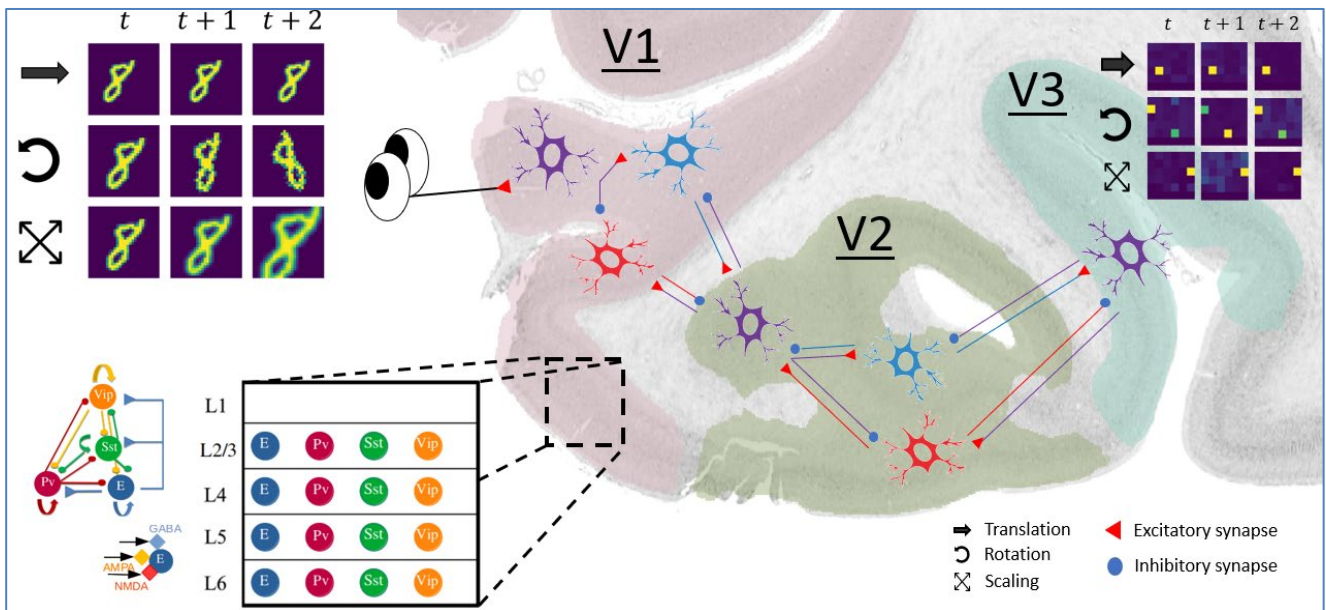


Figure 2: Showcase 4 - Development highlights and convergence of computational models of sensory predictions and object recognition.

Showcase 4 presents an integrative suite of three complementary models that investigate sensory predictions and object recognition at different levels of biological detail: 1) a neurobiological model (lower left) incorporates mouse connectivity data and includes detailed postsynaptic dynamics (AMPA, NMDA and GABA-A) to simulate spiking cortical columns of four neuron types (pyramidal, E; three interneuron types, PV, SST, and VIP); 2) a cognitive model uses rate-based neurons and predictive coding architecture that learns invariant representations of visual objects from temporal continuity (e.g. translation, rotation, and scaling; upper left and right); and 3) a hybrid model introduces spiking neurons and feedforward gist to predictive coding architecture to implement biologically plausible algorithms for learning hierarchical latent representations of a visual scene (e.g. V1 to V3; middle, superimposed on human visual cortex)

Project Number:	945539	Project Title:	HBP SGA3
Document Title:	Showcase 3 - DEMO3.2 and Showcase 4 - DEMO4.2		
Document Filename:	D2.3 (D14) SGA3 M21 ACCEPTED 220520.docx		
Deliverable Number:	SGA3 D2.3 (D14)		
Deliverable Type:	Demonstrator		
Dissemination Level:	PU = Public		
Planned Delivery Date:	SGA3 M21 / 31 Dec 2021		
Actual Delivery Date:	SGA3 M22 / 21 Jan 2022; accepted 20 May 2022		
Author(s):	Alain DESTEXHE, CNRS (P10) Cyriel PENNARTZ, UVA (P98)		
Compiled by:	Patricia CARVAJAL-VALLEJOS, IDIBAPS (P93), (Section 1) Angelica DA SILVA LANTYER, UVA (P98), (Section 2) Kwangjun LEE, UVA (P98), (Section 2)		
Contributor(s):	Núria TORT-COLET, CNRS (P10), contributed to Section 1 Rodrigo COFRE-TORRES, CNRS (P10), contributed to Section 1 Kevin ANCOURT, CNRS (P10), contributed to Section 1 David ACQUILUE, CNRS (P10), contributed to Section 1 Jennifer GOLDMAN, CNRS (P10), contributed to Section 1 Alain DESTEXHE, CNRS (P10), contributed to Section 1 Cyriel PENNARTZ, UVA (P98), contributed to Section 2 Jorge MEJIAS, UVA (P98), contributed to Section 2 Kwangjun LEE, UVA (P98), contributed to Section 2 Matthias BRUCKLACHER, UVA (P98), contributed to Section 2 Giulia MORENI, UVA (P98), contributed to Section 2		
WP QC Review:	Pier Stanislao PAOLUCCI, INFN (P92)		
WP Leader / Deputy Leader Sign Off:	Mavi SANCHEZ-VIVES, IDIBAPS (P93)		
T7.4 QC Review:	Martin TELEFONT, Annemieke MICHELS, EBRAINS (P1)		
Description in GA:	Advanced large scale, full brain simulation corresponding to different brain states and consciousness levels and robot demonstration and simulation of object and scene recognition v2.		
Abstract:	In Showcase 3, we demonstrate the simulation of states of unconsciousness in three species, including human, mouse, and monkey associated with the augmentation of spike-frequency adaptation, regulated naturally during the sleep-wake cycle. In particular, we show that both empirically observed spontaneous and evoked dynamics can be simulated using anatomical and connectivity data from all three species. Further, we deliver progress in simulating states of anaesthesia, varying parameters related to the hyperpolarisation of neuronal populations, a general mechanism on which all anaesthetic agents, regardless of their specific molecular		

<p>actions, converge. Finally, we deliver advancements in the multi-scale, TVB-AdEx model of human brain, in which each mean-field represents a vertex, approaching the resolution of a cortical column, with resolution much finer than in the previously delivered region-based model. In accompanying videos, we begin to see the emergence of spatially localised propagating waves in response to perturbations. These findings demonstrate the universality of slow waves between species, and also between different mechanisms generating unconsciousness.</p> <p>In Showcase 4, we are starting to combine predictive coding models of perception with the dynamics and neuronal circuitry characteristic of the cortex. To this end, we developed an integrative suite of three complementary models with different levels of biological realism: a neurobiological model of spiking cortical columns, a cognitive model of object-invariant perception, and a hybrid model of a predictive coding based spiking neural network. In Showcase 4, we present the highlights of their development and elaborate how integration of knowledge gained from these models can improve our understanding of perception, and brain diseases.</p>	<p>actions, converge. Finally, we deliver advancements in the multi-scale, TVB-AdEx model of human brain, in which each mean-field represents a vertex, approaching the resolution of a cortical column, with resolution much finer than in the previously delivered region-based model. In accompanying videos, we begin to see the emergence of spatially localised propagating waves in response to perturbations. These findings demonstrate the universality of slow waves between species, and also between different mechanisms generating unconsciousness.</p> <p>In Showcase 4, we are starting to combine predictive coding models of perception with the dynamics and neuronal circuitry characteristic of the cortex. To this end, we developed an integrative suite of three complementary models with different levels of biological realism: a neurobiological model of spiking cortical columns, a cognitive model of object-invariant perception, and a hybrid model of a predictive coding based spiking neural network. In Showcase 4, we present the highlights of their development and elaborate how integration of knowledge gained from these models can improve our understanding of perception, and brain diseases.</p>
Keywords:	Mean-field model, AdEX neurons, full-brain simulations, human neural activity, connectome, tractography, Homo sapiens (human), Mus musculus (mouse), Macaca mulatta (macaque), brain states, consciousness, sleep, anaesthesia, predictive coding, perception, object recognition, spiking neural network, object invariance, cortical columns, biophysical model.
Target Users/Readers:	Computational neuroscience community, computer scientists, Consortium members, HPC community, neuroimaging community, anaesthesiologists, neurologists, cognitive neuroscientists, physicists, neuroinformaticians, funders, neuroscientists, platform users, researchers, general public.

Table of Contents

1. Showcase 3: Brain Complexity and Consciousness, Demo 2	5
1.1 Introduction	5
1.2 Technical Specification	5
1.2.1 Mouse model of wake and slow-wave states	6
1.2.2 Macaque model of wake and slow-wave states	9
1.2.3 Human model of wake and slow-wave states	12
1.2.4 Study of oscillatory states in human model	12
1.2.5 Human model at higher resolution	13
1.3 How to access the Showcase	15
1.3.1 Showcase 3 Demo V2 video	15
1.3.2 Access to models of spontaneous activity	15
1.3.3 Access to tutorials in EBRAINS for the calculation of PCI	15
1.3.4 Access to short videos of different brain states on different species	15
1.4 Looking Forward	16
1.5 References	16
2. Showcase 4: Perception and Recognition of Objects and Scenes, Demo 2	18
2.1 Introduction	18
2.2 Technical Specification	19
2.2.1 Hybrid model: spiking neural network for predictive coding	19
2.2.2 Cognitive model: predictive coding to learn invariant representations of visual objects from temporal continuity	21
2.2.3 Neurobiological model: spiking cortical column	21
2.3 How to access the Showcase	23
2.3.1 Showcase 4 Demo V2 video	23
2.3.2 Access to code for the models	23
2.4 Looking Forward	23
2.5 References	24

Table of Figures

Figure 1: Showcase 3 - Simulation of brain states in mouse, macaque and human. Whole-brain simulations of wake-like (conscious) and anaesthesia (unconscious) states in three different species.	1
Figure 2: Showcase 4 - Development highlights and convergence of computational models of sensory predictions and object recognition.	1
Figure 3: Complexity of the multiunit activity response to a stimulus on the mouse at different levels of anaesthesia. Adapted from Dasilva et al., 2021.	6
Figure 4: Spontaneous wide-field calcium signal during intermediate or deep anaesthesia.	6
Figure 5: Complexity of the wide-field calcium imaging data during intermediate or deep anaesthesia. ...	7
Figure 6: Spontaneous calcium activity of the mouse TVB model during different brain states.	7
Figure 7: Complexity of the calcium response during different brain states.	8
Figure 8: Functional connectivity at different brain states.	8
Figure 9: Macaque Brain in TVB.	9
Figure 10: Simulations of the Macaque Brain showing asynchronous state and synchronous states.	9
Figure 11: Power spectrums of asynchronous and synchronous states.....	10
Figure 12: Functional connectivity matrices of asynchronous and synchronous states.....	10
Figure 13: Synchronous regime through hyperpolarisation.	10
Figure 14: Power spectra for synchronous states generated by hyperpolarisation.	11
Figure 15: Synchronous functional connectivities due to hyperpolarisation	11
Figure 16: Experimental al simulated bold-like functional connectivity of awake macaques.....	11
Figure 17: Experimental and simulated bold-like functional connectivity of anaesthetised macaques.....	12
Figure 18: Trend to lower complexity of responsiveness in anaesthetised-like state compared to conscious-like state.....	12
Figure 19: Oscillatory states emerging at intermediate levels of spike-frequency adaptation.	13
Figure 20: Simulation of light and deep anaesthesia in the human surface brain model, with 14,982 vertices.	13
Figure 21: Simulation of spontaneous activity in the human brain with the surface model.	14
Figure 22: Simulation of evoked activity in the human brain with the surface model.	14
Figure 23: Spiking neural network for predictive coding (SNN-PC).....	20
Figure 24: Predictive coding on dynamic input sequences.	22
Figure 25: Graphical representation of spiking cortical column model.....	22

1. Showcase 3: Brain Complexity and Consciousness, Demo 2

1.1 Introduction

Understanding consciousness is one of the grand challenges of contemporary neuroscience. Why does it fade and recover during transitions across physiological, pharmacological and pathological brain states? How can we determine whether a behaviourally unresponsive patient is conscious? Can we quantify consciousness levels? Can we use our multi-scale understanding of brain-state transitions to devise strategies to induce recovery of consciousness? A brain-based quantification of the levels of consciousness is of the utmost importance because, each year, intensive care medicine is called upon to treat millions of patients whose level of consciousness is difficult to assess due to severe brain injuries and disconnections. Detecting the fundamental mechanisms of consciousness is crucial, not only for better diagnosis, but also to guide recovery in an optimal manner. Finally, it is critical to provide tools - such as eye tracking or brain computer interfaces - to provide communication channels for patients who have recovered consciousness but remain disconnected (e.g. locked-in patients). Another relevant requirement comes from the field of anaesthesiology - pharmacologically induced alterations of consciousness - which is used in millions of patients every year. The effectiveness of this approach is limited by a lack of systematic understanding of the underlying circuit mechanisms and a lack of reliable brain-based measures of anaesthesia depth. Therefore, deeper understanding of consciousness also paves the way to engineering novel methods of tracking the results of pharmacological interventions, as well as engineering next-generation, non-pharmaceutical, direct methods for inducing states of non-responsiveness, with potentially fewer side effects and dangers.

In the previous Demo 3.1 (See SGA3 Deliverable D2.1 (M9): [Showcase 3 - DEMO3.1 and Showcase 4 - DEMO4.1¹](#)), we demonstrated that the implementation of AdEx mean-field models (developed in SGA2) into the Virtual Brain (TVB) leads to a framework where one can evaluate the effect of “microscopic” parameters, such as spike-frequency adaptation, on the “macroscopic” behaviour at the level of the whole brain, such as the emergence of synchronised slow waves. We could replicate the TMS-EEG (Transcranial Magnetic Stimulation - Electroencephalography) experiments done in the wake-sleep cycle in humans (Goldman et al., 2021).

In this second Showcase Demo 3.2, we extend such simulations of full brain activity to anaesthetised states, during spontaneous activity and after stimulation. Stimulation results in perturbed or evoked activity, with spatiotemporal interactions between areas that have a different fingerprint, corresponding to different brain states. These brain states can be physiological (sleep or awake), as shown before, but also pharmacological (e.g. anaesthesia levels), or due to disorders of consciousness (e.g. traumatic brain injury). For these reasons, we have used the simulation capabilities offered by the Human Brain Project’s (HBP’s) EBRAINS neuroscience research infrastructure to make access to the models as wide as possible. The simulations delivered here at SGA3 Month 22 (January 2022) illustrate how emergent patterns of activity can be reproduced in silico and shed light on their microscopic underpinnings. These simulations are presented with qualitative and quantitative analyses pioneered in empirical data, for direct comparison to activity recorded during different brain states in three species: human subjects, macaque monkey and mouse.

1.2 Technical Specification

We show here simulations of the whole-brain model, for mouse, macaque and monkey. We show both spontaneous activity (asynchronous and slow-wave states), and evoked activity. In each species

¹ https://sos-ch-dk-2.exo.io/public-website-production/filer_public/f8/b3/f8b31220-1d29-4d6f-a30a-5ae0eb01d871/d21_d12_sga3_m9_accepted_210504.pdf

we aim to simulate how evoked responses depend on brain state, with an emphasis on anaesthesia. Our models investigate how the loss of consciousness (induced by anaesthetics) influences the propagation of information, and more generally, how the brain processes external inputs.

1.2.1 Mouse model of wake and slow-wave states

We start by showing the experimental evaluation and modelling of perturbational complexity index (PCI) in the mouse, recorded using extracellular electrodes. This first experimental data set (Dasilva et al., 2021) consists of the same electric stimuli delivered in different states of anaesthesia (Figure 3), showing that the PCI inversely follows the depth of anaesthesia (Figure 4).

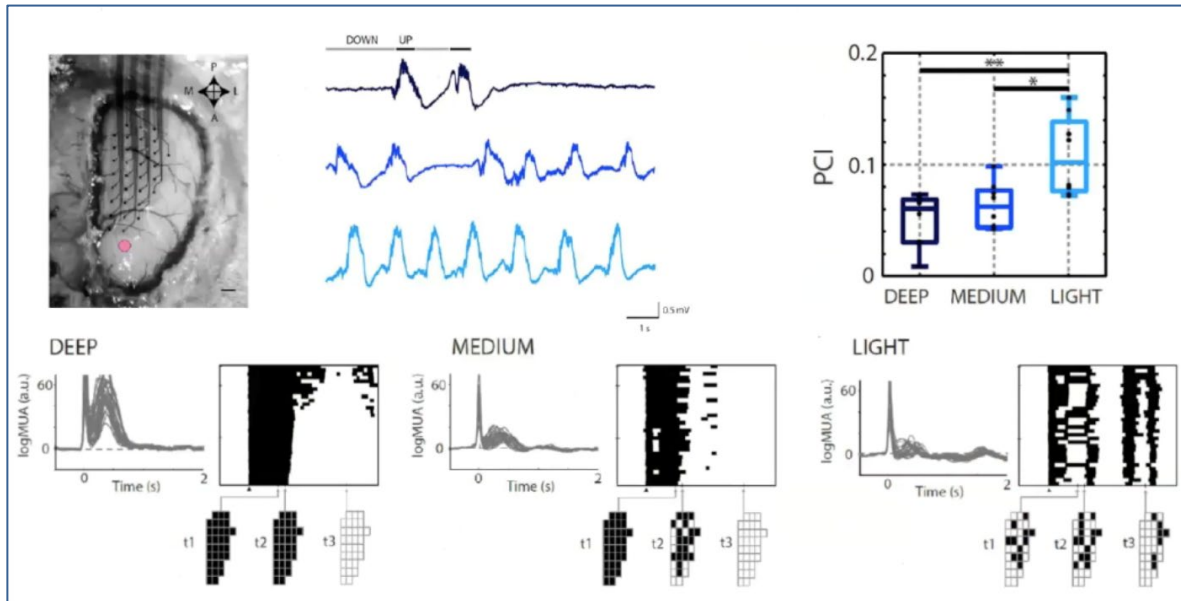


Figure 3: Complexity of the multiunit activity response to a stimulus on the mouse at different levels of anaesthesia. Adapted from Dasilva et al., 2021.

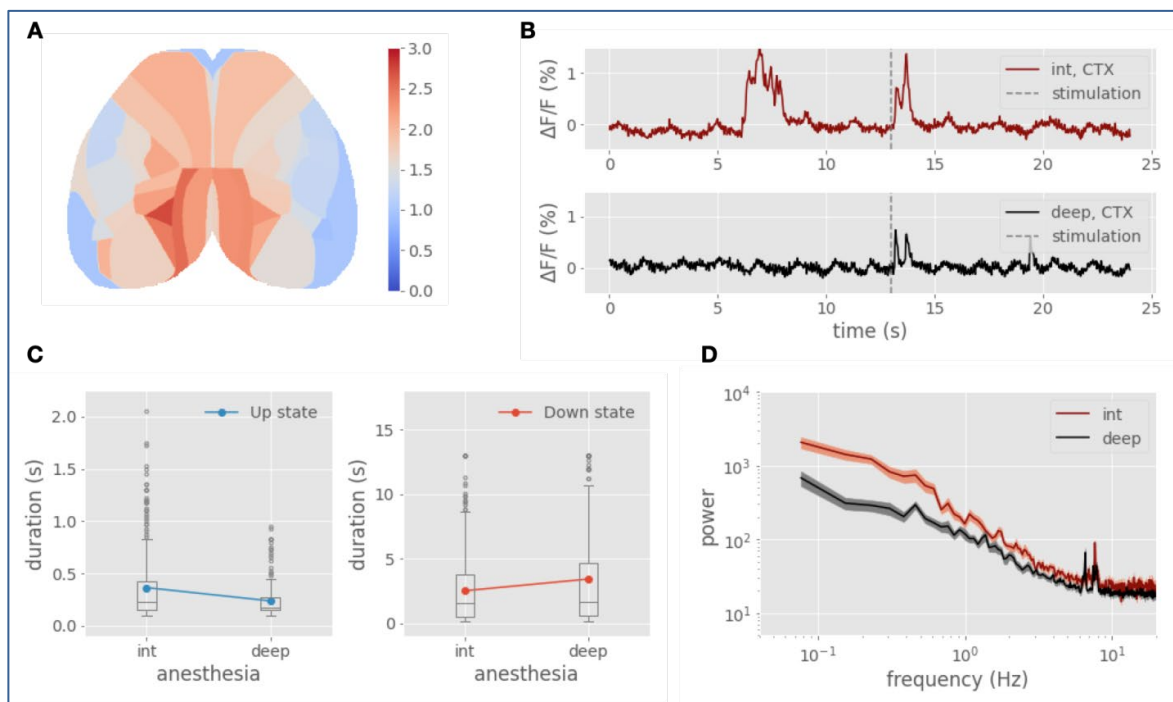


Figure 4: Spontaneous wide-field calcium signal during intermediate or deep anaesthesia.

A. Snapshot of the activity of the different cortical areas, colour code is the intensity of the fluorescence. B. Example traces of the averaged activity over all the cortical areas in each level of anaesthesia, before and after stimulation. C. Changes in duration of Up or Down states when increasing the level of anaesthesia. Data from $n=4$ subjects. D. Power spectral densities of the average of the cortical signal across trials and subjects.

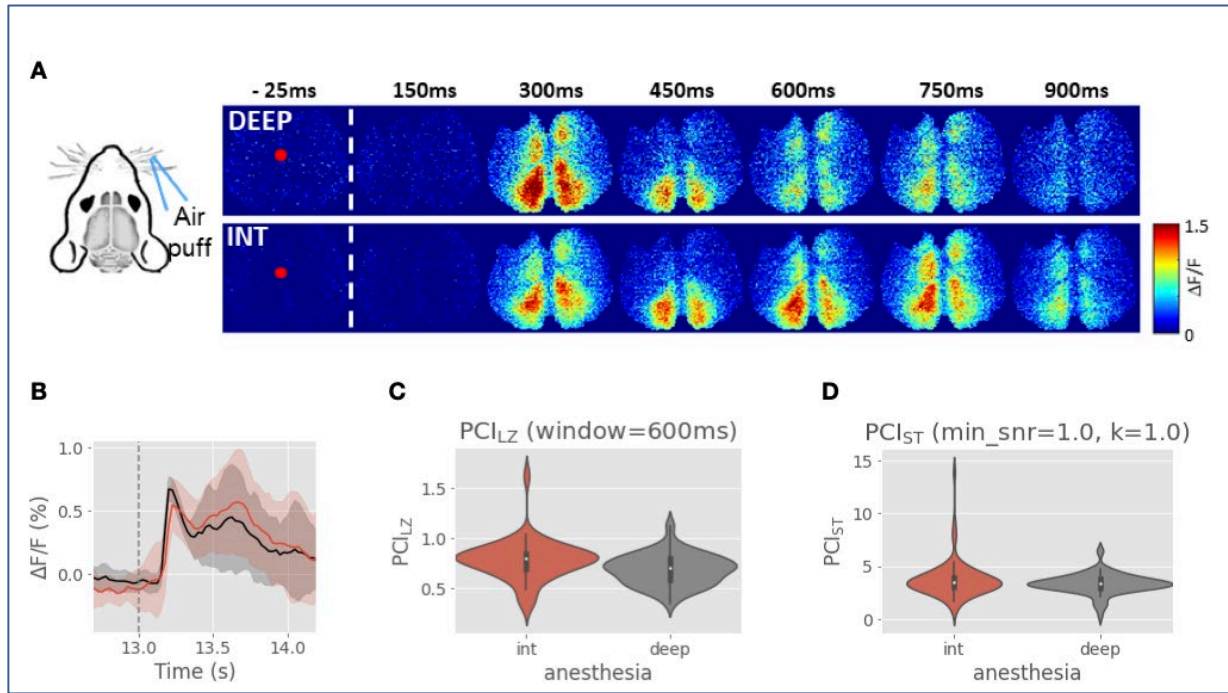


Figure 5: Complexity of the wide-field calcium imaging data during intermediate or deep anaesthesia.

A. Snapshots of the activity of the cortex during the response to a whisker stimulation in deep (top) or intermediate (bottom) anaesthesia, colour code is the intensity of the fluorescence. B. Example of the average response of the cortex across trials in one subject during intermediate (red) or deep (black) anaesthesia. C. Complexity of the response in each condition measured using PCI_{LZ} . D. Complexity of the response in each condition measured using PCI_{ST} .

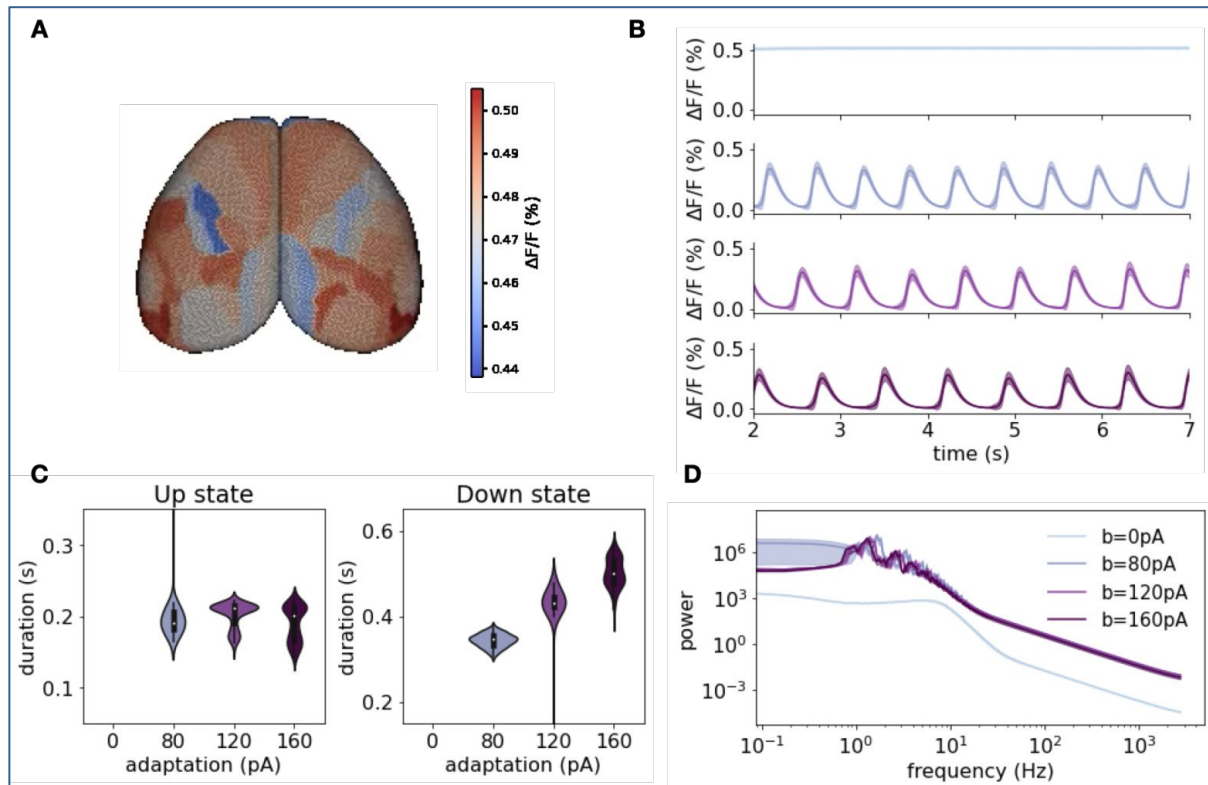


Figure 6: Spontaneous calcium activity of the mouse TVB model during different brain states.

A. Snapshot of the activity of the different cortical areas. Colour code is the intensity of the fluorescence. B. Example traces of the averaged activity over all the cortical areas in each brain state: from wakefulness (top) to deep anaesthesia (bottom) by increasing the strength of adaptation (parameter b in the model). Same legend as in panel D. C. Changes in duration of Up or Down states when increasing the level of adaptation. D. Power spectral densities of the average of the cortical signals at each brain state (mean and standard deviation over realisations). Data from $n=20$ realisations of each condition.

Another set of data from LENS (Allegra et al., unpublished) consists of a similar protocol, recorded in calcium imaging, which also show the same trend (Figure 5).

To model these data, we have considered the TVB simulation environment where we integrated the AdEx mean-field model with adaptation (di Volo et al., 2019). As shown previously, the TVB-Adex model can simulate slow-waves, which were provided here for mouse and calcium imaging signals (Figure 6). We estimated the PCI (Figure 7) and the functional connectivity in this model (Figure 8).

Interestingly, the state-dependent PCI (PCI_{ST}) did not display the trend found experimentally, but the Lempel-Ziv PCI (PCI_{LZ}) provided simulations in perfect agreement with experiments (Figure 7).

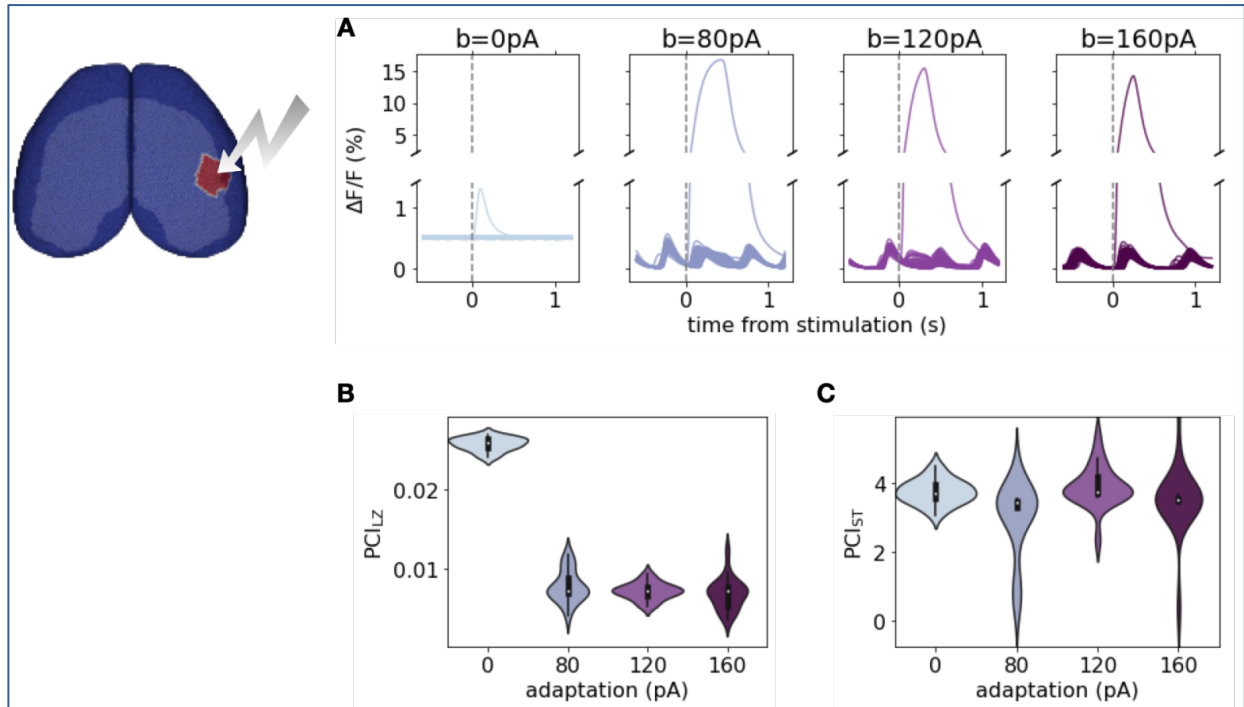


Figure 7: Complexity of the calcium response during different brain states.

A. Response to a 60ms stimulation of the barrel field cortex in different brain states, from wakefulness to deep anaesthesia as modelled by increasing adaptation strength (b parameter). The Y axis is broken to show the full response of the stimulated area (top) and the smaller response of the remaining cortical areas (bottom). B. Complexity of the response in each condition measured using PCI_{LZ} . C. Complexity of the response in each condition measured using PCI_{ST} . Data from $n=20$ realisations of each condition.

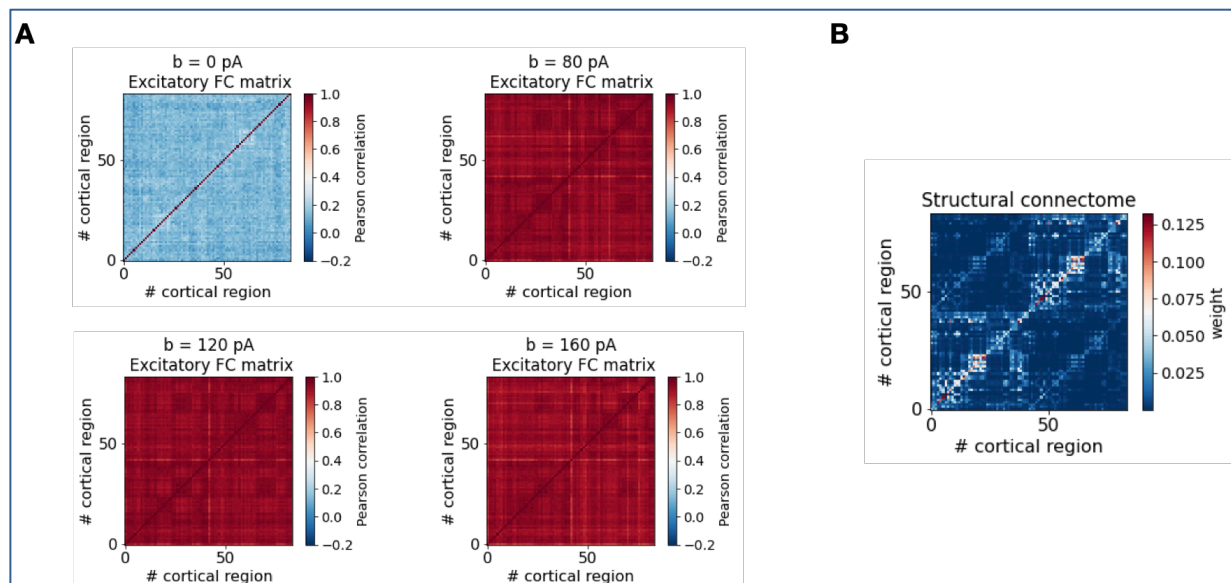


Figure 8: Functional connectivity at different brain states.

A. Functional connectivity matrices at each level of consciousness showing an increase of pairwise correlations for synchronous states. B. Structural connectome of the mouse model.

1.2.2 Macaque model of wake and slow-wave states

Next, we considered TVB simulations of the macaque brain (Figure 9). Similarly to human and mouse, the macaque TVB-AdEx model displayed asynchronous and slow-wave states (Figure 10, Figure 11). The evaluation of the functional connectivity (Figure 12) gave very different patterns in these two states. The response to stimuli, and the associated PCI, are in progress experimentally, and were not yet attempted in the model - they will be reported later.

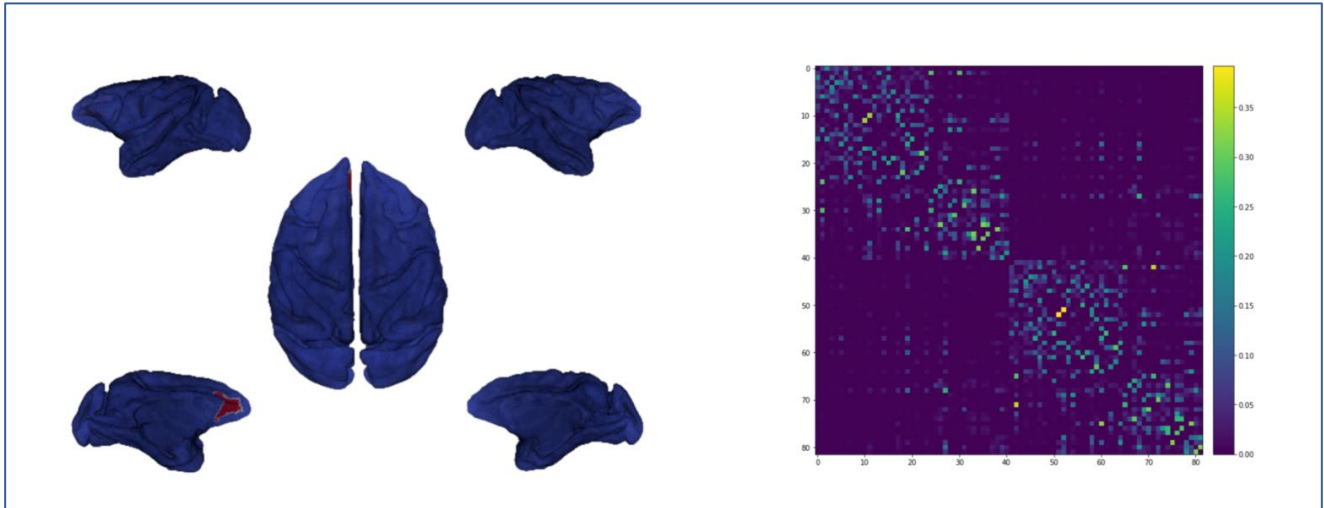


Figure 9: Macaque Brain in TVB.

We used the macaque brain implemented in TVB. In particular, we used the COCOMAC connectome to run simulations of the AdEx mean-field model.

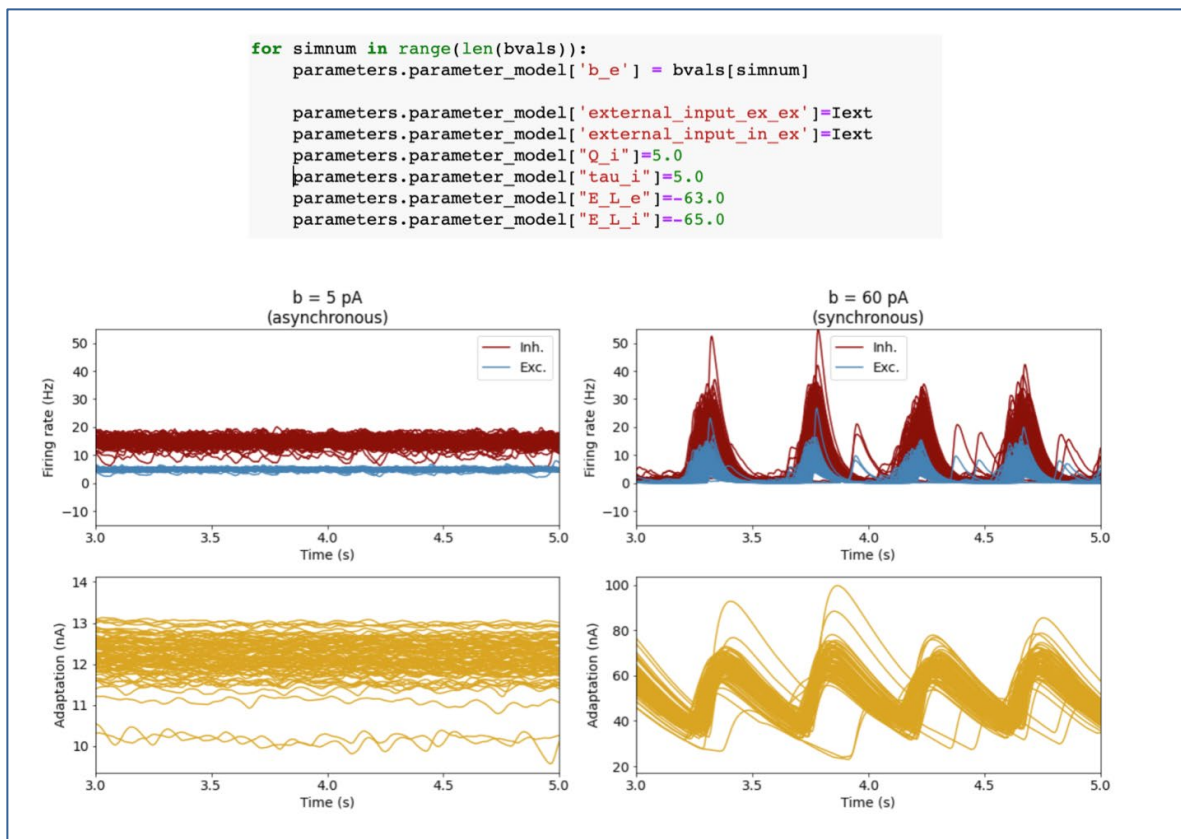


Figure 10: Simulations of the Macaque Brain showing asynchronous state and synchronous states.

Moving the spike frequency adaptation parameter from $b=5$ to $b=60$, we transit from an asynchronous state that models awake consciousness to a synchronous state that models sleep states.

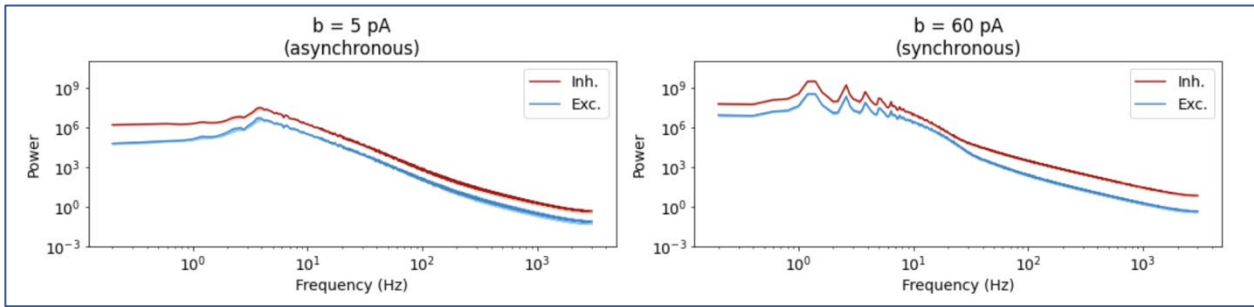


Figure 11: Power spectrums of asynchronous and synchronous states.

When the spike frequency adaptation parameter is set to $b=5$ we observe a single peak 6Hz in contrast to what we observe at $b=60$, where several peaks appear and the more pronounced ones are in the slow-wave regime.

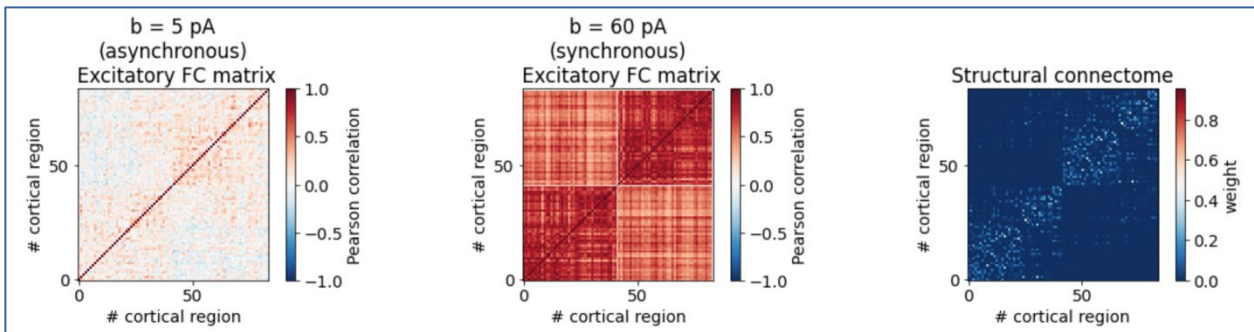


Figure 12: Functional connectivity matrices of asynchronous and synchronous states.

In the asynchronous regime the functional connectivity matrix shows values close to zero showing no significant pairwise correlation between nodes. In the synchronous regime, we observe more pronounced correlations.

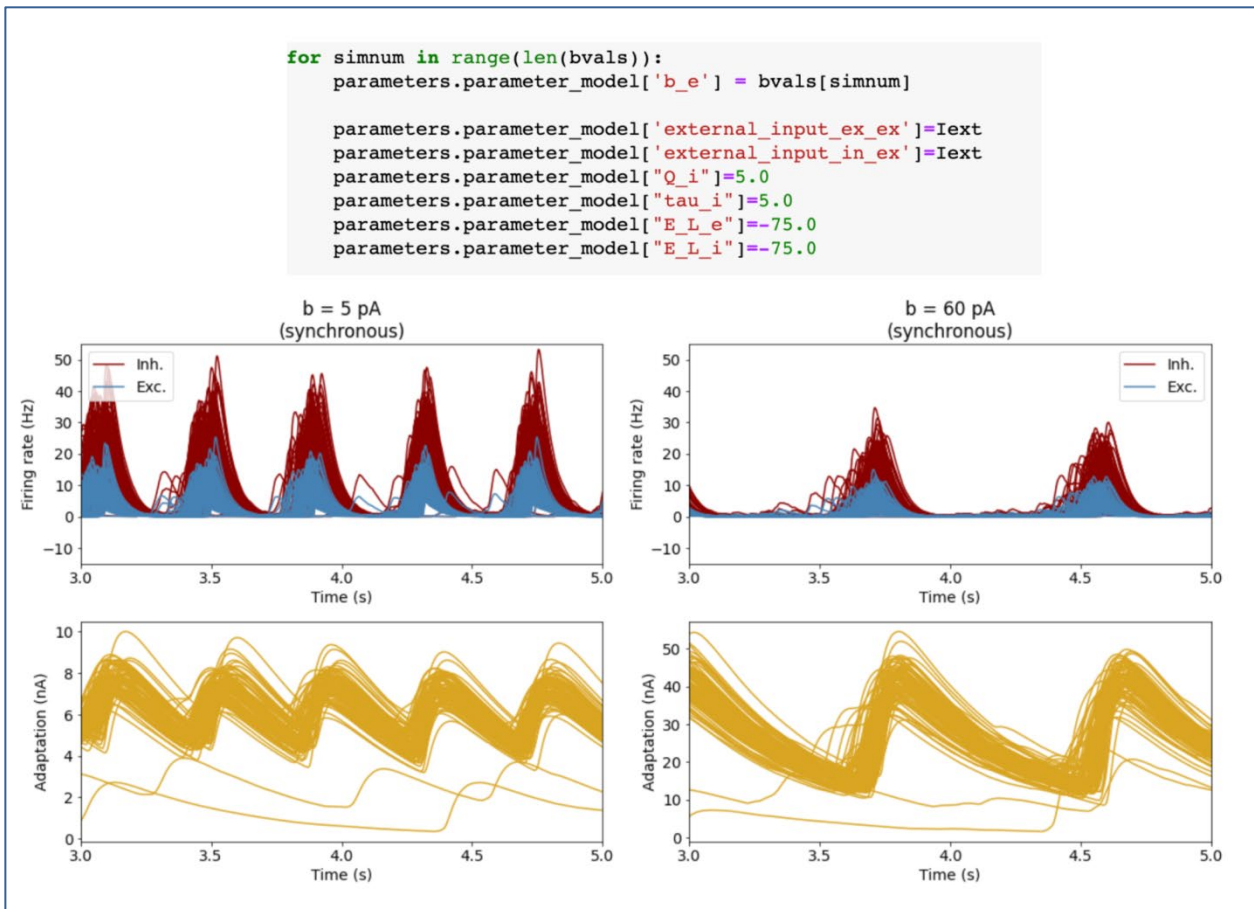


Figure 13: Synchronous regime through hyperpolarisation.

The synchronous regime can be generated by hyperpolarising cells. In this example, we transit from excitatory and inhibitory reversal potentials of -63mV and -65mV respectively to -75mV and -75mV respectively.

Regarding the effect of anaesthetics, the model exhibited slow waves arising from hyperpolarisation (Figure 13 and Figure 14; see Figure 15 for functional connectivity). We also simulated the BOLD signal in the macaque TVB-AdEx model (Figure 16, Figure 17), which will allow future comparison with fMRI data in macaque (work in progress).

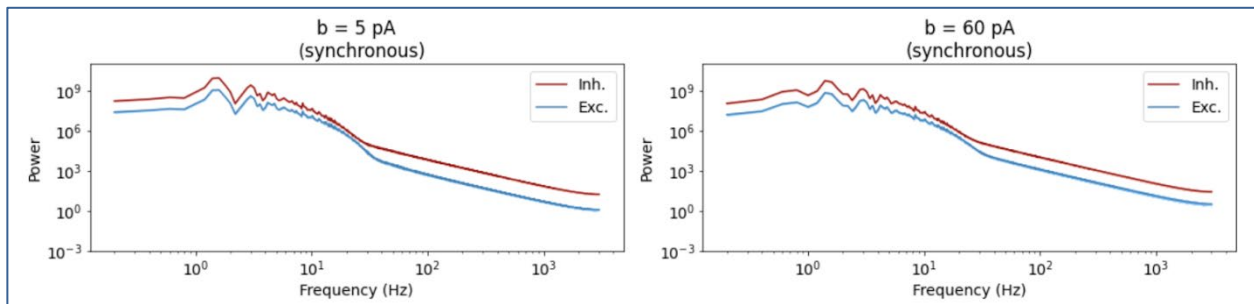


Figure 14: Power spectra for synchronous states generated by hyperpolarisation.

When the spike frequency adaptation parameter is set to $b=5$, we observe several peaks, the more pronounced one near 3 Hz. For $b=60$, we observe several peaks and the more pronounced is near 1 Hz.

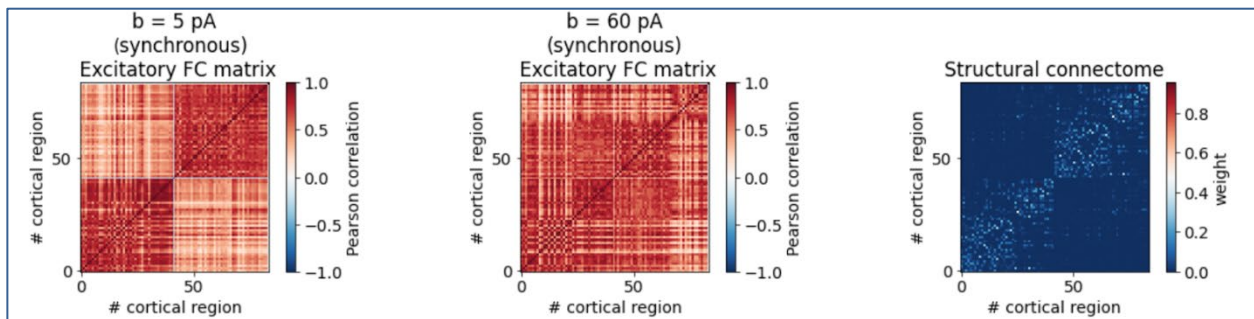


Figure 15: Synchronous functional connectivities due to hyperpolarisation

Here, for both spike frequency adaptation values $b=5$ and $b=60$, we observe high values of pairwise correlations.

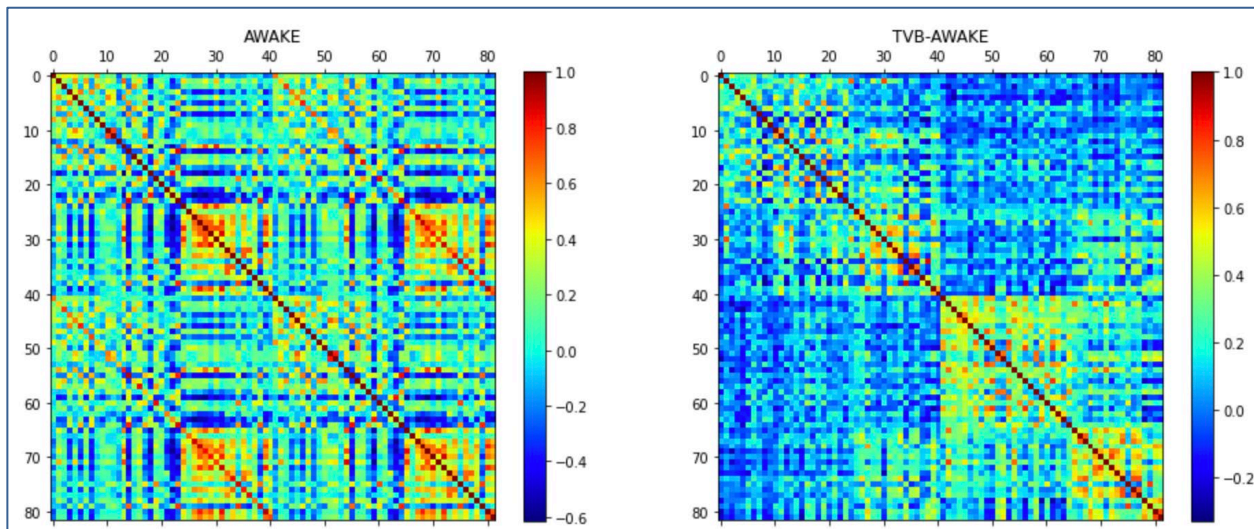


Figure 16: Experimental and simulated bold-like functional connectivity of awake macaques

Left: functional connectivity obtained from experimental fMRI data of awake macaques in resting state. Right: we simulate Bold-like signals using TVB and the COCOMAC connectome using the parameters that generate asynchronous firing rate.

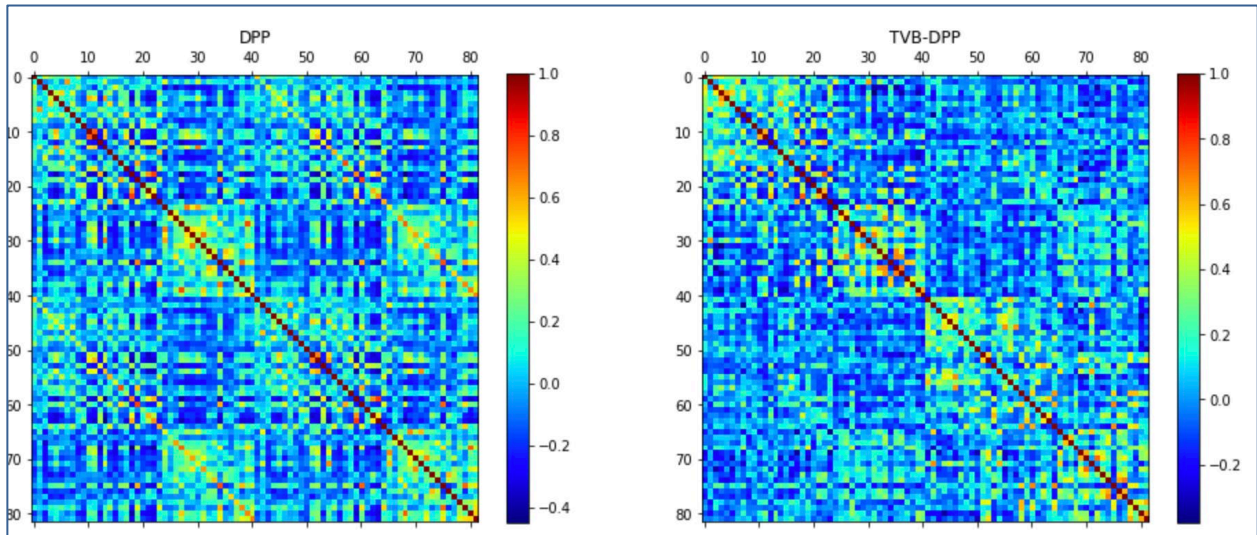


Figure 17: Experimental and simulated bold-like functional connectivity of anaesthetised macaques

Left: functional connectivity obtained from experimental fMRI data of anaesthetised macaques using propofol. Right: simulated functional connectivity of Bold-like signals using TVB and the COCOMAC connectome using the parameters that generate synchronous firing rate.

1.2.3 Human model of wake and slow-wave states

The TVB-AdEx model was also used in human, where we could also simulate the emergence of slow waves with hyperpolarisation (not shown; see below). Here, the PCI was evaluated and showed lower values in anaesthesia (Figure 18).

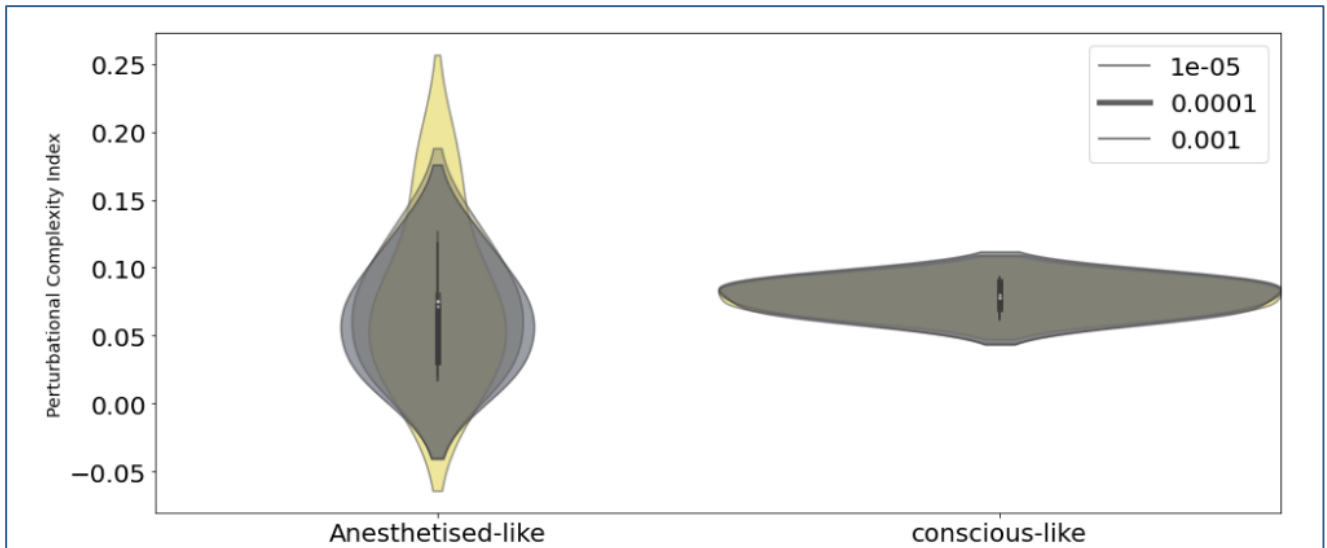


Figure 18: Trend to lower complexity of responsiveness in anaesthetised-like state compared to conscious-like state.

Perturbational complexity index in the human whole-brain, region-based model, comparing an anaesthesia-like (left) to an awake-like (right) regime. 5 realisations are included in the analysis for each condition. Parameters changed to achieve the anaesthesia-like regime $E_{le} = E_{li} = -75$, $b=5$, whereas in the awake-like regime, $E_{le} = -65$, $E_{li} = -63$, and $b=5$. These results show a convergence to reduced responsiveness by hyperpolarising the neuronal populations, a general mechanism shared by anaesthetics.

1.2.4 Study of oscillatory states in human model

To further understand the repertoire of oscillatory states in the TVB-AdEx model, we studied the various parameters that allow the emergence of oscillations (Figure 19). This study revealed that

besides asynchronous and slow-wave (Up/Down) states, a third state appears under the form of limit cycle oscillations. These oscillations occur for intermediate levels of spike frequency adaptation.

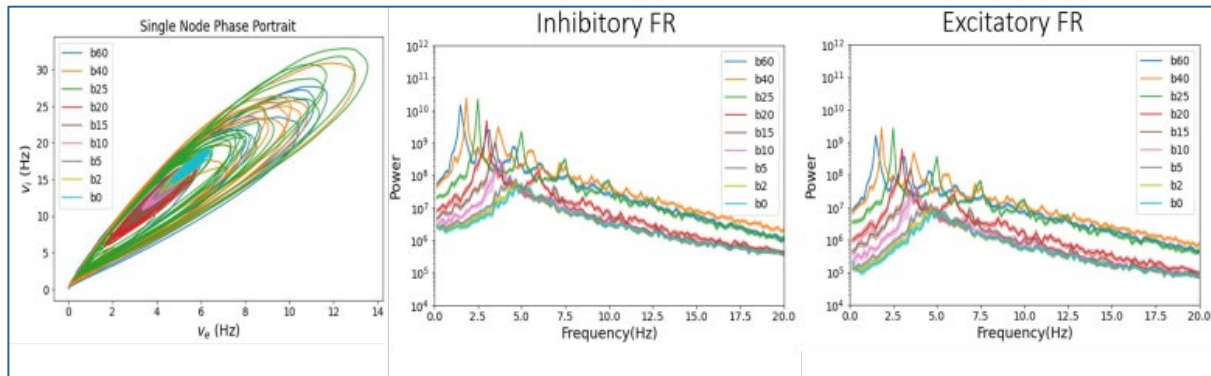


Figure 19: Oscillatory states emerging at intermediate levels of spike-frequency adaptation.

On the left, exploration of intermediate values of spike frequency adaptation strength (parameter b) showing the presence of a fixed point for values of $b=0, 2$, and 5 , but limit cycles emerging for intermediate values of b , and bistable regimes observed for high values of b . In middle and right panels, the power spectra show a smooth transition of the power maxima, which shifts continuously rightward (to higher frequencies) with decreasing amounts of spike frequency adaptation, as expected (Dasilva et al., 2021, Tort-Colet et al., 2021).

1.2.5 Human model at higher resolution

Finally, we have investigated a new TVB model, characterised by a high resolution voxelisation of cerebral cortex, called the “surface-based model”. When equipped with the AdEx mean-fields, this model can also simulate Wake-Sleep-like states (Figure 20) and anaesthesia-like states (Figure 21) and their response to external stimuli (Figure 22). In addition, the surface-based TVB-AdEx model exhibits travelling wave activity at mesoscale (see videos in Section 1.3).

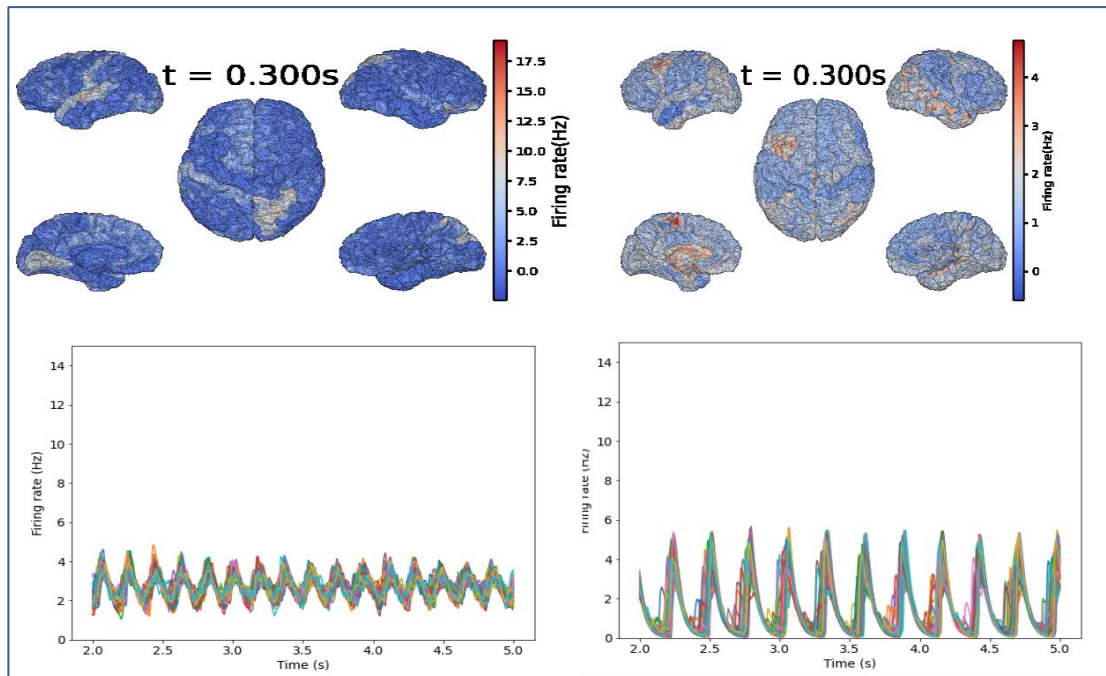


Figure 20: Simulation of light and deep anaesthesia in the human surface brain model, with 14,982 vertices.

(Top) Firing rate of 50 randomly selected nodes in a human brain surface simulation showing spontaneous activity. To simulate light anaesthesia, the spike-frequency adaptation was slightly increased to $b=5$, the delay τ_i was increased to 7 to mimic longer GABAergic channel open time, and the membrane potentials of the nodes were hyperpolarised to $E_{L_e} = E_{L_i} = -75$. Here we see the emergence of a limit cycle. (Bottom). Firing rate of a human brain simulation with the surface model and a spontaneous activity. To simulate a deep anaesthesia, spike-frequency adaptation was increased to $b=40$, the delay τ_i was increased to 10, and $E_{L_e} = E_{L_i} = -80$ for the hyperpolarisation of nodes.

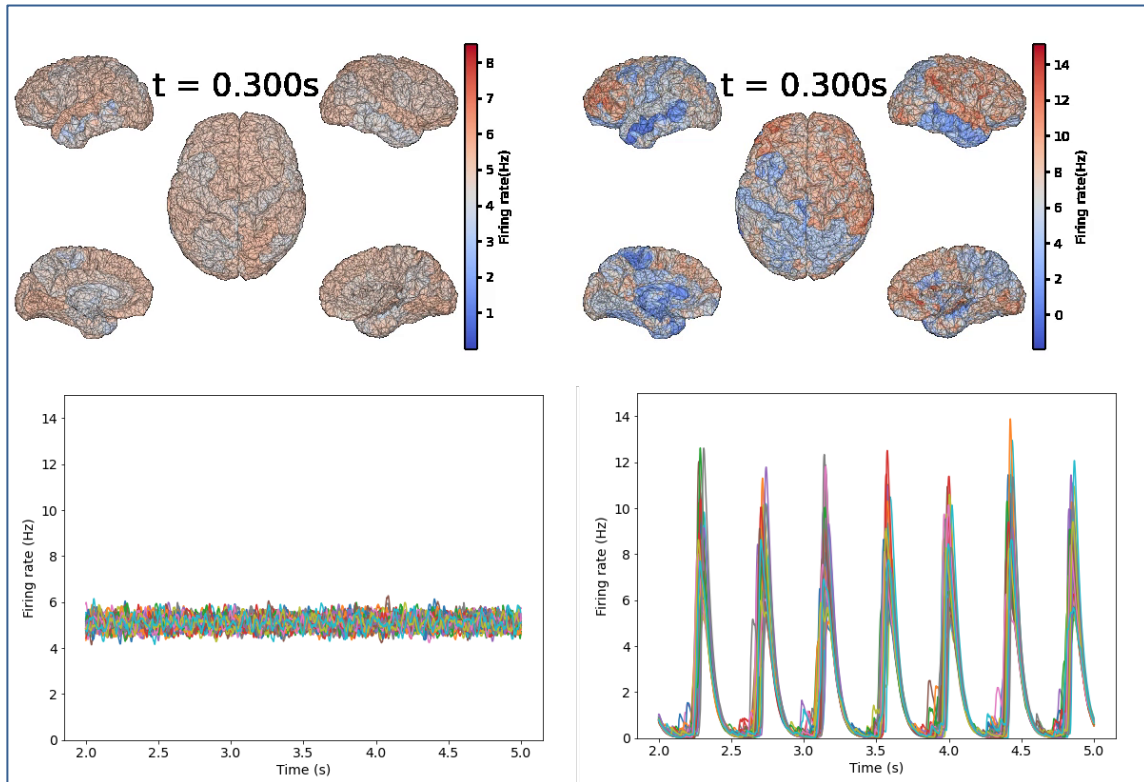


Figure 21: Simulation of spontaneous activity in the human brain with the surface model.

(Left) Firing rate of a human brain simulation with the surface model and a spontaneous activity. The spike-frequency adaptation (b) value is equal to 5 and we display only 50 random nodes out of the 14,982 contained in the surface model. (Right) Firing rate with $b = 60$ and same 50 vertices.

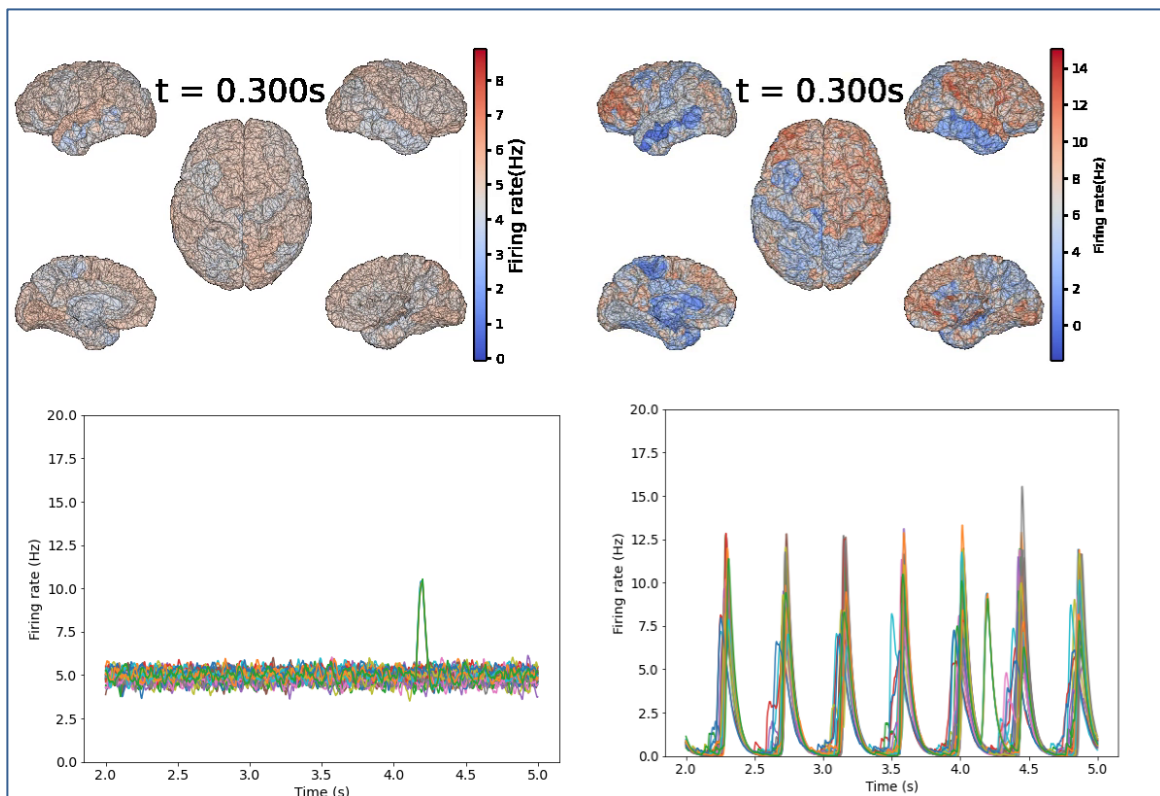


Figure 22: Simulation of evoked activity in the human brain with the surface model.

(Left) Firing rate of neuronal populations in the surface-based human brain simulation. A stimulus is given at 4.25s to the right caudal middle frontal gyrus. The spike-frequency adaptation (b) value is equal to 5 and 50. Randomly selected nodes are displayed, some of which belong to the stimulated region. The stimulus is equal to 0.0001 Hz. (Right) Firing rate with $b = 60$, showing the same vertices responding to the same perturbation.

1.3 How to access the Showcase

1.3.1 *Showcase 3 Demo V2 video*

The Showcase 3 output is a video entitled: "Simulations of the complexity of evoked brain responses in different states of consciousness" (<https://youtu.be/IP9NPwHwmTU>) that introduces the motivation and background of our research and summarises the results obtained in the three species, as described here.

1.3.2 *Access to models of spontaneous activity*

To access the three species models of spontaneous activity, the following tutorials are available in EBRAINS:

- For the mouse: <https://drive.ebrains.eu/f/c9913afb062f472688f8/>
- For the human: <https://drive.ebrains.eu/f/781625de8ce14989ba98/>
- For the macaque: <https://drive.ebrains.eu/f/ded8f918007d4c97b579/>
- For the human surface: <https://drive.ebrains.eu/u/d/fb8953a5441d46ce80ba/>

1.3.3 *Access to tutorials in EBRAINS for the calculation of PCI*

There are two tutorials in EBRAINS for the calculation of PCI:

Calculation of PCI in the mouse calcium TVB model at different levels of consciousness available at the following link: <https://drive.ebrains.eu/f/4e3f129852444f789e9a/>

Calculation of PCI in the human brain available in the following link: <https://drive.ebrains.eu/f/c7b04ecf744049359595/>

1.3.4 *Access to short videos of different brain states on different species*

- For the mouse “awake” (b=0pA): <https://drive.ebrains.eu/f/c412e190a4bb46f3b7dc/>
- For the mouse “anesthetized” (b=60pA): <https://drive.ebrains.eu/f/c3788843033640c9b067/>
- For the human “Anesthetized” (b=5pA): <https://drive.ebrains.eu/f/7da2a9b79e264614b6c7/>
- For the human “Anesthetized” (b=40pA): <https://drive.ebrains.eu/f/e246952d785c4b6e945a/>
- For the human “Spontaneous awake-like”(b=5pA):
<https://drive.ebrains.eu/f/22413e3d769a4cf0ac12/>
- For the human “Spontaneous activity sleeping-like” (b=60pA):
<https://drive.ebrains.eu/f/b2fa2fb3daec4ce4a1a4/>
- For the human “Evoked activity awake-like” (b=5pA):
<https://drive.ebrains.eu/f/56a3d9a3db7748108969/>
- For the human “Evoked activity awake-like” (b=60pA):
<https://drive.ebrains.eu/f/7b4de92c14c2467a8a3b/>
- For the macaque “awake - Asynchronous” (b=0pA):
<https://drive.ebrains.eu/f/81d27af467ca45c5966d/>

- For the macaque “anesthetized - Synchronous” (b=60pA):
- <https://drive.ebrains.eu/f/df5d3c95a2ef4e769a34/>

Despite the simplicity of the code used, some of the jupyter notebooks provided above have a memory demand that is higher than that provided by EBRAINS. Due to this fact, the kernel might restart even if the code runs well in a local computer. We expect to solve this issue in the following weeks or months.

1.4 Looking Forward

This work contributes to several areas of active work in the HBP. Firstly, it contributes to modelling, because it is the first time biophysical network models (with sophisticated biophysical features such as adaptation and conductance-based interactions) have contributed to “biologically-realistic” mean-field models (displaying several activity states). These models are integrated in EBRAINS to simulate, with computationally non-demanding methods, large-scale network-level (whole brain) simulations. Three distinct scales of modelling are thus integrated here: microscopic (network of neurons), mesoscopic (mean-field), and macroscopic (whole-brain). Secondly, this Showcase contributes to knowledge of Brain States, because the models simulate different brain states, from high consciousness brain states such as wakefulness to several levels of low consciousness brain states (anaesthesia or sleep-like) with synchronised dynamics. Thirdly, this Deliverable contributes to research in Cognitive Function because the model captures how information about stimuli are integrated by different brain areas, a situation which occurs uniquely in asynchronous states, consistent with the high-level sensory integration displayed by the brain in the awake state. Finally, the model delivered here is useful for contributing to knowledge of changes in dynamical complexity between brain states and helps identify mechanisms relating changes in relationships between structural and functional connectivity between different states.

This work is of broad interest to computational neuroscientists, anaesthesiologists, neurologists, cognitive neuroscientists, and physicists. The generality of the tools offered by this Deliverable are due to the enormous flexibility of the models displayed in the Showcase that offer the means to connect knowledge of brain function across spatio-temporal scales and identify microscopic mechanisms as key to physiological changes in global brain networks.

This Showcase is relevant for several downstream purposes. Firstly, this work is delivered in a manner consistent with the requirements of high-performance computing (HPC), allowing the scaling up of models to more detailed, higher-resolution representations of human brain activity, representations of personalised multi-scale brain activity, as well as parameter exploration and bifurcation analyses. These downstream HPC applications will enrich specific knowledge of individual variation in brain activity related to healthy and abnormal brain states. As such, this work will also bear clinical interest, as we will use the models delivered here to investigate states of consciousness, which will be used as a companion to better understand the results of empirical analyses of spontaneous human brain activity as well as that evoked by sensory stimuli and TMS stimulation in various brain states (in conjunction with HBP Work Package WP1).

The next steps will be to investigate brain states with vanishing levels of consciousness. Besides sleep states investigated last year, and the states of anaesthesia investigated here, we plan to continue towards studying states of coma and minimal consciousness, as well as pathological states such as epilepsy and stroke if time permits. This will be done with data from our colleagues in the HBP. We will also pursue a similar approach as outlined here for mouse and macaque brain, using measurements such as EcoG, Ca imaging and fMRI.

1.5 References

- Dasilva, M., Camassa, A., Navarro-Guzman, A., Pazienti, A., Perez-Mendez, L., Zamora-López, G., ... & Sanchez-Vives, M. V. (2021). Modulation of cortical slow oscillations and complexity across anesthesia levels. *Neuroimage*, 224, 117415. **P2595**.

- Tort-Colet, N., Capone, C., Sanchez-Vives, M. V., & Mattia, M. (2021). Attractor competition enriches cortical dynamics during awakening from anesthesia. *Cell Reports*, 35(12), 109270. **P2976**.
- Di Volo M, Romagnoni A, Capone C and Destexhe A. (2019) Biologically-realistic mean-field models of conductance-based networks of spiking neurons with adaptation. *Neural Comput.* 31: 653-680. doi: https://doi.org/10.1162/neco_a_01173. **P1864**.
- Goldman JS, Kusch L, Hazal Yalcinkaya B, Depannemaecker D, Nghiem TA, Jirsa V and Destexhe A. (2021) A comprehensive neural simulation of slow-wave sleep and highly responsive wakefulness dynamics. *BioRxiv* 2021.08.31.458365; doi: <https://doi.org/10.1101/2021.08.31.458365>. **P3023**.

2. Showcase 4: Perception and Recognition of Objects and Scenes, Demo 2

2.1 Introduction

In the previous Demo 4.1 (See SGA3 Deliverable D2.1 (M9): [Showcase 3 - DEMO3.1 and Showcase 4 - DEMO4.1](#)²), we demonstrated a successful implementation of predictive coding-based deep neural network model (MultiPredNet; Dora et al., 2021) on a rodent-like biomimetic robot and its counterpart on the EBRAINS virtual robotics platform (Whisk-Eye robot; <https://www.youtube.com/watch?v=0blgdAE1cbk>). The model and robot were able to integrate visual and tactile information gathered from a head-mounted camera and 24 artificial whiskers to perform autonomous navigation. This work was extended during the Demo 4.2 and is in press for publication (Pearson et al., 2021).

For the second Demo 4.2, our goal was to elaborate on these models to build predictive coding models of perception which can be integrated with models of the dynamics, circuitry and neuronal spiking mechanisms of the cortex. More specifically, Showcase 4 progressed to provide highlights of three computational models (currently in further development) that aim to implement different levels of biological realism: 1) a neurobiological/cognitive hybrid model, which is constructed with a biologically realistic neuron model (i.e. spiking neuron) and a local learning rule (i.e. Hebbian learning) to perform object reconstruction; 2) a cognitive model, which is built with rate-based neurons to focus on extending the cognitive ability of the hybrid model by introducing movement invariance; and 3) a neurobiological model, which simulates a realistic spiking cortical column using available connectivity data from the literature and Knowledge Graph. Integrating the knowledge gained from the three models can improve the understanding of perception and sensory predictions, offer valuable insights in neural mechanisms of brain disorders such as autism or schizophrenia, and inspire neuromorphic and robotic applications.

The models make use of and contribute to the EBRAINS Research Infrastructure (RI). The neurobiological model uses anatomical data from the Knowledge Graph and other external datasets, such as the Allen Institute for Brain Science, to estimate the connection strengths and probabilities derived from mouse visual cortex. In collaboration with NEST developers, the novel feature of the neurobiological model, exact postsynaptic NMDA receptor dynamics, is incorporated into an existing Simulation service tool (i.e. NEST) and is currently under further development by the NEST team. It also uses a Simulation service tool, ViSimpl, to visualise the spatial and temporal features of spiking cortical columns. The hybrid model also uses Community service of the EBRAINS Research Infrastructure (RI). Given our successful application for FENIX computing and storage resources, the hybrid model is trained to generate internal representations of visual input on a supercomputer (CSCS Piz Daint). In collaboration with the Scientific Liaison Unit (SLU), we plan to implement the hybrid model on the EBRAINS RI and add it to the list of Simulation service models. With intuitive GUIs, novice users will be able to run example simulations with a pre-trained version of the hybrid model. Advanced users or researchers in relevant fields can conduct sustainable simulations using the embedded model and compare their results with other models listed in the Simulation service.

Given the generative nature of both cognitive and hybrid models, they have the potential for a wide range of downstream applications that can benefit from efficient learning of sensory inputs (e.g. AI, prostheses, robotics, etc.), as now demonstrated for the WhiskEye robot (see below and Pearson et al., 2021). Meanwhile, the local learning of connection weights and the asynchronous, event-driven activities of the spiking hybrid model can also contribute to the development of energy-efficient neuromorphic computing.

Additionally, based on work described in SGA3 Deliverable D2.1, we further developed our deep network model for predictive coding which is now able to integrate information across sensory

² https://sos-ch-dk-2.exo.io/public-website-production/filer_public/f8/b3/f8b31220-1d29-4d6f-a30a-5ae0eb01d871/d21_d12_sga3_m9_accepted_210504.pdf

modalities (Pearson et al., 2021), to provide clues for better understanding how the brain generates consciousness, given that conscious experience has been argued to be based on a large-scale, internally generated representation of the world and body. In particular, the strong positive correlation found between pose and representation spaces inferred by the trained multi-sensory deep predictive coding network (MultiPredNet) has been developed further using the NRP. The original arena used for Showcase 4.1 (see SGA3 Deliverable D2.1) has been expanded in size and sensory richness for longer duration excursions of the WhiskEye simulated in the NRP of EBRAINS. This work has confirmed that the original statistical correlation between the two spaces is maintained in larger, more complex visual-tactile environments. We also demonstrated that, when coupled to a simple memory system, it can be used to robustly detect loop closure events sufficient for the robot to localise itself (Pearson et al., 2021). WP3 collaborates with WP2 to focus on bio-plausible navigation. Thus, this robot demonstration project has led to uptake by WP3 and significant collaboration between WP2 and WP3. Specifically, the MultiPredNet and WhiskEye model in the NRP have been integrated with a spiking neural network model of rodent head direction cells. MultiPredNet now learns to associate natural visual scenes with the spike-based representation of head direction via the joint latent layer. Once trained, the network is capable of reconstructing a representation of head direction inferred from visual cues that can be used to inject a corrective signal into the head direction cell populations based on a coupled ring attractor network. The spiking network model is simulated using NEST whilst the MultiPredNet relies on the TensorFlow library coupled to the WhiskEye model within the NRP. Using this apparatus, we have conducted cue-conflict experiments to compare the spike response of our model to biological measurements taken from rodents experiencing similar conditions.

2.2 Technical Specification

The following section is divided into three subsections, each of which corresponds to one of the three computational models we developed and provides technical details. We note that the integration of these models into an expanded cognitive-neurobiological cortical architecture is planned for the next phase.

2.2.1 *Hybrid model: spiking neural network for predictive coding*

In order to account for the biological plausibility of predictive coding models, we developed a spiking neural network for predictive coding (SNN-PC, Figure 23), in which neurons communicate with event-driven, asynchronous spikes instead of the non-linear, continuous, and clock-driven function approximator (i.e. a rate-based neuron) used in standard artificial neural networks. Our SNN-PC inherits the algorithmic legacies of previous predictive coding (PC) neural network models (Rao & Ballard, 1999; Dora et al., 2021), which infer the causes of sensory inputs via hierarchical interactions between error-computing and prediction-generating neurons and update the generative model for prediction using a form of Hebbian learning. In addition, we have introduced two novel features that further improve biological plausibility in the model. First, we introduce a direct fast feedforward pathway, constituted by sparse projections from input to higher layers, which generates and quickly transmits an abstract representation of input (i.e. a neural code for the gist of a scene). This provides a neurobiological alternative to arbitrary sample - or class-specific priors which are commonly used by other models. Second, we specifically consider two separate classes of error units, viz. positive and negative error-computing neurons, which better reflects the neurobiological constraint following from Dale's principle (which states that a neuron's outgoing projections are all either excitatory or inhibitory). After training with the hand-written digit dataset MNIST, SNN-PC was able to develop hierarchical latent representations and make inferences about the causes of samples it had not seen during training, as visualised by correct digit reconstruction. We used

In the first semester of 2022, we plan to extend the model to a more realistic predictive-coding microcircuit model which explicitly incorporates differentiated types of inhibitory cells (such as PV, SST and VIP cells) and incorporate circuit-level dynamics, which will be an important step towards the final integrated cognitive-neurobiological model. We will continue to utilise the allocated EBRAINS HPC resource for the model development.

2.2.2 Cognitive model: predictive coding to learn invariant representations of visual objects from temporal continuity

To examine how a network of recurrently organised neurons may infer invariant object representations, we trained a predictive coding network (Rao & Ballard, 1999; Dora et al., 2021) on sequences of moving MNIST digits. Contrary to the case of the hybrid model above, this model (Figure 24) uses simplified rate units to simulate neural activity, which allows us to focus on the complex computations underlying object representations with spatial invariance properties. Development of such representations is mediated purely by Hebbian learning which links slowly varying predictions from higher network levels (“object identity”) to different sensory patterns (“observed features”). As representations in lower areas of the network are driven both by bottom-up sensory input and top-down predictions, trained networks can complete occluded parts of previously observed scenes when presented with a sequence of a digit gradually disappearing behind a dark screen. Such behaviour is in line with observed decodability of occluded scene areas from activity patterns in early visual regions (Smith & Muckli, 2010). Overall, the proposed learning paradigm generalises predictive coding from static to dynamic inputs in a novel and more biologically plausible way than networks that learn to predict forward in time through backpropagation of self-supervised error-gradients (Lotter et al., 2016). Our approach may both give a plausible explanation for learning and inference of invariant object representations and accounts for experimental evidence for top-down predictions where sensory input is scarce (Smith & Muckli, 2010). Next steps will be to extend the model with the capacity to perceive motion through motion detectors. This is expected to allow a) segmenting a moving object from its background (or vice versa) and b) allow feedback from these motion detectors to be used as spatiotemporal predictions. Soon, models will be trained on the high-performance computing systems of HBP/EBRAINS resources within the FENIX infrastructure⁴. Results will be integrated with the biophysically more realistic models of 2.2.1 and 2.2.3 to extend the capability of these detailed models to more complex cognitive tasks. After publication, the integrated model will be added to the EBRAINS Knowledge Graph to facilitate interaction of other researchers with the simulation.

2.2.3 Neurobiological model: spiking cortical column

To complement the two models above and extend our understanding of predictive coding principles towards more neurobiologically realistic frameworks, we built a computational model of a cortical column in the visual cortex. The model was constrained using neuroanatomical and electrophysiological data and constitutes our first step towards a biophysically detailed model of object recognition under predictive coding principles. In order to develop such a model, we used available connectivity data from the literature (including, for example, openly available connectivity datasets from the Allen Institute for Brain Science (Billeh et al., 2020)) and Knowledge Graph. In particular, the current model (Figure 25) is based on average synaptic strengths and connection probabilities across four cell types (pyramidal, PV, SST and VIP neurons) observed in the cortical column of mouse V1. The model incorporates a laminar structure by including real cell-specific densities per layer and laminar connection strength and probabilities, and includes detailed post-synaptic receptors dynamics for AMPA, NMDA and GABA-A. The first version of the model was entirely

⁴ We acknowledge the use of Fenix Infrastructure resources, which are partially funded from the European Union Horizon 2020 research and innovation programme through the ICEI project under Grant Agreement No. 800858.

built in Nest, a powerful simulator for spiking neural network models. Part of the simulations to understand the dynamics of the cortical column were performed using this tool. Then using ViSimpl we were able to develop a 3D visualisation of the column showing the level of activity of the different neuron types. By adjusting the influence of surrounding neurons to the ones in our network, we showed that the model can reproduce realistic levels of neural firing activity under spontaneous and stimulus-evolved conditions, taken from in vivo electrophysiological recordings (Billeh et al., 2020). In the upcoming months, we plan to study the effects of external input (both bottom-up and top-down) in the network, calculate the simulated local field potentials corresponding to the network activity, and incorporate plasticity rules to allow modifications of the synaptic weights.

In this next stage to upscale the model and perform fast simulations we will need HBP resources such as High Performing Computer (HPC). The model will build an important bridge between cellular models of cortical columns and perceptual function.

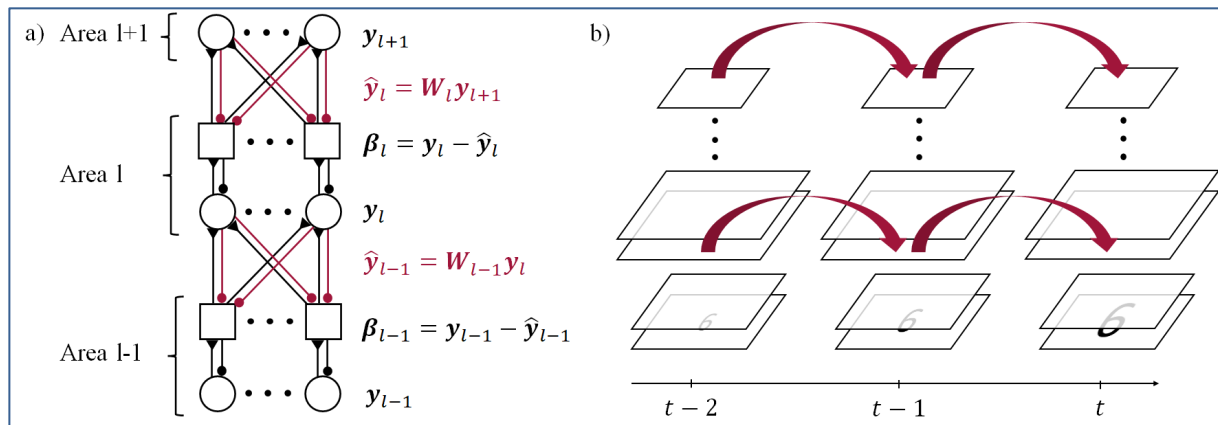


Figure 24: Predictive coding on dynamic input sequences.

a) Rate-based predictive coding architecture. y denotes the representational activities in each layer that send down the descending predictions \hat{y} that are multiplied with the synaptic weights W . β denotes the error neuron activities. b) Inference on sequential input images (digit 6, of varying size in a looming movement scenario) are fed to the lowest network area and are represented at different levels of the processing hierarchy. Neural activity is maintained in all areas except the input area from one timestep to the next (red arrows).

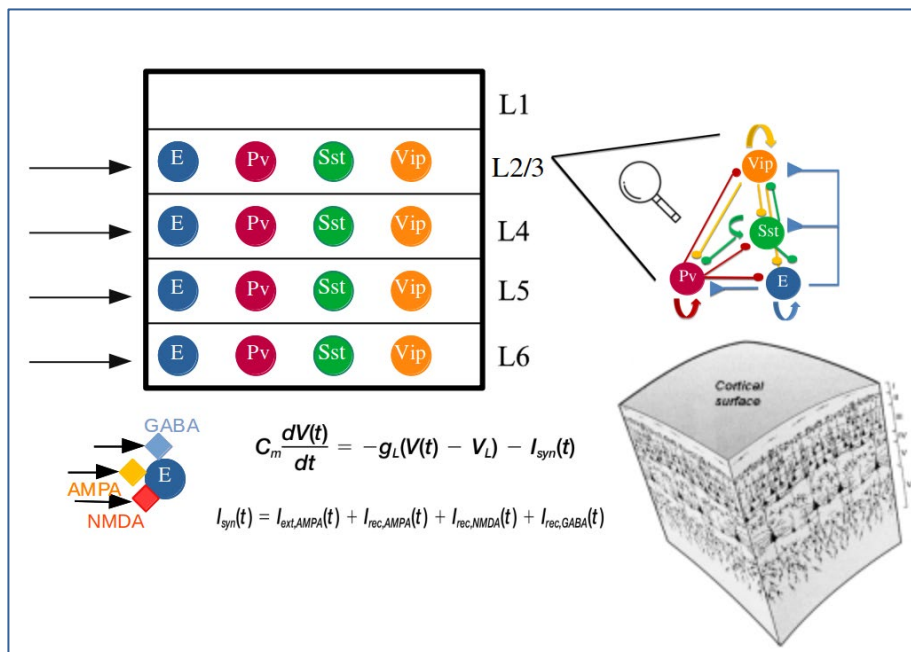


Figure 25: Graphical representation of spiking cortical column model.

In each layer excitatory neurons (E), and 3 inhibitory neuron types are present (PV, SST, VIP). Each neuron receives inputs from the other neurons through 3 distinct receptors (NMDA and AMPA receptors for excitatory connections and GABAA receptors for inhibitory connections). Each ionotropic receptor is modelled with its own distinct dynamics.

2.3 How to access the Showcase

2.3.1 Showcase 4 Demo V2 video

The Showcase 4 Output is a video entitled: A suite of models for visual perception and invariant object recognition (<https://youtu.be/zaon2KDLBjs>) that introduces the motivation and background of our research and summarises the three models (2.2.1, 2.2.2 and 2.2.3) at a level that can be understood by both lay audiences and scientific communities.

2.3.2 Access to code for the models

The neural network (Dora et al., 2021) and robotics implementations (Knowles et al., 2021) of our work have been published and can be accessed via the following link: <https://search.kg.ebrains.eu/instances/2164c2b9bbb66b42ce358d108b5081ce>.

The deep neural network model for predictive coding with Hebbian learning (Dora et al., 2021) has been published and can be accessed via the following link (soon to be incorporated to EBRAINS): <https://github.com/shirindora/DGHPC>

The example code for the hybrid model will be uploaded to EBRAINS in the first semester of 2022. Codes for the cognitive and neurobiological models are still under development and will be uploaded to EBRAINS as soon as they fulfil the necessary efficiency and reproducibility requirements.

The information about the novel feature incorporated to the NEST simulation in relation to the neurobiological model is currently under development by the NEST team. The current code can be accessed via this link: https://github.com/stinebuu/nest-simulator/tree/nmda_model_wang

2.4 Looking Forward

So far, we have described the different computational models of sensory predictions and object recognition (from neurobiologically detailed to cognitive oriented to hybrid versions) and established the basis to do so in neurobiologically detailed models. The goal of the research illustrated in Showcase 4, however, is to integrate the knowledge we gain with each of these models.

In the first semester of 2022, the three models will be further developed in parallel, and they will start to converge in certain aspects. First, Lee et al. will build a modified spiking model at the hybrid level which will be closer to the neurobiological model while conserving the achieved properties for object recognition in predictive coding. In particular, the new hybrid model will incorporate the different cell types which are already present in the cortical column model (i.e. pyramidal neurons, PV, SST and VIP cells). This will allow us to explore the role of these cell types in SNN-PC, and to make predictions about the consequences of, for example, optogenetically silencing specific cell types in predictive coding computations.

Second, the cognitive model will advance to incorporate mechanisms to perceive motion using motion detectors. This will be an important step to allow the model to discriminate between a moving object and its static background, and therefore perform a figure-background segregation operation, as observed experimentally (Self et al., 2015). This will also permit the feedback signals from these motion detectors to be used as spatiotemporal predictions.

Third, the neurobiological model will incorporate realistic learning rules to allow for activity-dependent changes in synaptic weights of both excitatory and inhibitory neurons. In particular, the incorporation of plasticity rules will allow us to extend the model towards multiarea networks, so that we can simulate storing of high-level object representations in cortical areas higher in the hierarchy (resembling the ‘ventral stream’ model of object recognition). The presence of NMDA receptors, which have been successfully introduced in the current version of the model, will play a major role in the ability of long-term encoding of neural representations. This will then lead us to

test our hypothesis for object recognition under predictive coding in a highly detailed neurobiological framework.

In addition to these converging efforts, WP1 and EBRAINS will provide intuitive GUI support for the hybrid (2.2.1) and the neurobiological models (2.2.3; e.g. by using visualisation tools such as VISimpl, which we used to display the preliminary results of the neurobiological models in the Demo V2 video), through which users of any level of expertise can readily establish better understanding of the model and judge its potential use cases in the upcoming months.

It is worth to mention that the three models will be entered in the Knowledge Graph by the end of HBP SGA3.

2.5 References

- Billeh YN et al. (2020). Systematic Integration of Structural and Functional Data into Multi-scale Models of Mouse Primary Visual Cortex. *Neuron* 106, pp. 388-403.
- Földiák P (1991). Learning invariance from transformation sequences. *Neural Comput.* 3.2, pp. 194-200.
- Lotter W, Kreiman G and Cox D (2016). A neural network trained for prediction mimics diverse features of biological neurons and perception. In: *Nat. Mach. Intell.* 2.4, pp. 210-219.
- Dora S, Bohte SM and Pennartz CMA (2021). Deep Gated Hebbian Predictive Coding Accounts for Emergence of Complex Neural Response Properties Along the Visual Cortical Hierarchy. In: *Front. Comput. Neurosci.* Jul 28;15:666131. PMID: 34393744; PMCID: PMC8355371. **P2878.**
- Pearson MJ, Dora D, Struckmeier O, Knowles TC, Mitchinson B, Tiwari K, Kyrki V, Bohte S and Pennartz CMA (2021). Multimodal representation learning for place recognition using Deep Hebbian predictive coding. In: *Frontiers in Robotics and AI.* **P3027.**
- Rao R and Ballard D (1999). Predictive coding in the visual cortex: a functional interpretation of some extra-classical receptive-field effects. In: *Nat Neurosci* 2, pp. 79-87.
- Self MW, Mookhoek A, Tjalma T and Roelfsema PR (2015). Contextual effects on perceived contrast: Figure-ground assignment and orientation contrast. In: *Journal of vision* 15 (2), 2-2.
- Smith FW and Muckli L (2010). Nonstimulated early visual areas carry information about surrounding context. In: *Proc. Natl. Acad. Sci. USA* 107.46, pp. 20099-20103.
- Knowles TC, Stentiford R, Pearson MJ (2021) WhiskEye: A Biomimetic Model of Multisensory Spatial Memory Based on Sensory Reconstruction. In: Fox C., Gao J., Ghalamzan Esfahani A., Saaj M., Hanheide M., Parsons S. (eds) *Towards Autonomous Robotic Systems. TAROS 2021. Lecture Notes in Computer Science*, vol 13054. Springer, Cham. https://doi.org/10.1007/978-3-030-89177-0_43. **P3083.**